

Original Article

## *Notopterygium Incisum* Extract Promotes Apoptosis by Preventing the Degradation of BIM in Colorectal Cancer\*

Jun-he CHEN<sup>1</sup>, Cheng-ming WEI<sup>1</sup>, Qian-yu LIN<sup>1</sup>, Zi WANG<sup>1</sup>, Fu-ming ZHANG<sup>1</sup>, Mei-na SHI<sup>1</sup>, Wen-jian LAN<sup>2</sup>, Chang-gang SUN<sup>3</sup>, Wan-jun LIN<sup>1</sup>, Wen-zhe MA<sup>1#</sup>

<sup>1</sup>State Key Laboratory of Quality Research in Chinese Medicine, Macau University of Science and Technology, Macau 999078, China

<sup>2</sup>School of Pharmaceutical Sciences, Sun Yat-sen University, Guangzhou 510006, China

<sup>3</sup>College of Traditional Chinese Medicine, Weifang Medical University, Weifang 261053, China

© Huazhong University of Science and Technology 2024

**[Abstract] Objective:** Colorectal cancer (CRC), a prevalent malignancy worldwide, has prompted extensive research into anticancer drugs. Traditional Chinese medicinal materials offer promising avenues for cancer management due to their diverse pharmacological activities. This study investigated the effects of *Notopterygium incisum*, a traditional Chinese medicine named Qianghuo (QH), on CRC cells and the underlying mechanism. **Methods:** The sulforhodamine B assay and colony formation assay were employed to assess the effect of QH extract on the proliferation of CRC cell lines HCT116 and Caco-2. Propidium iodide (PI) staining was utilized to detect cell cycle progression, and PE Annexin V staining to detect apoptosis. Western blotting was conducted to examine the levels of apoptotic proteins, including B-cell lymphoma 2-interacting mediator of cell death (BIM), B-cell lymphoma 2 (Bcl-2), Bcl-2-associated X protein (BAX) and cleaved caspase-3, as well as BIM stability after treatment with the protein synthesis inhibitor cycloheximide. The expression of BAX was suppressed using lentivirus-mediated shRNA to validate the involvement of the BIM/BAX axis in QH-induced apoptosis. The *in vivo* effects of QH extract on tumor growth were observed using a xenograft model. Lastly, APC<sup>Min+</sup> mice were used to study the effects of QH extract on primary intestinal tumors. **Results:** QH extract exhibited significant *in vitro* anti-CRC activities evidenced by the inhibition of cell proliferation, perturbation of cell cycle progression, and induction of apoptosis. Mechanistically, QH extract significantly increased the stability of BIM proteins, which undergo rapid degradation under unstressed conditions. Knockdown of BAX, the downstream effector of BIM, significantly rescued QH-induced apoptosis. Furthermore, the *in vitro* effect of QH extract was recapitulated *in vivo*. QH extract significantly inhibited the tumor growth of HCT116 xenografts in nude mice and decreased the number of intestinal polyps in the APC<sup>Min+</sup> mice. **Conclusion:** QH extract promotes the apoptosis of CRC cells by preventing the degradation of BIM.

**Keywords:** *Notopterygium incisum*; colorectal cancer; apoptosis; B-cell lymphoma 2-interacting mediator of cell death

DOI <https://doi.org/10.1007/s11596-024-2883-1>

Colorectal cancer (CRC) is characterized by the malignant growth of cells in colon tissues. As the third most prevalent cancer worldwide, CRC carries a significant mortality burden<sup>[1]</sup>. Current clinical treatments for CRC include targeted drugs, surgery, and chemotherapy. However, the efficacy of these treatments is far from satisfactory, with low cure rates and a propensity for relapse noted. Additionally, some anti-CRC drugs cause severe toxicity, debilitate patients and reduce their quality of life. Consequently, effective drugs against CRC have always been desirable.

Traditional Chinese medicinal materials have received considerable attention in the field of anticancer research. The genus *Notopterygium incisum* is a perennial herb belonging to Umbelliferae, Apioidae, and Smyrnieae, and it is endemic to China. Within this genus, 5 plant species exist: *Notopterygium franchetii* H. de Bross, *Notopterygium incisum* Ting ex H.T. Chang,

*Notopterygium pinnatiinvolutum* Pu et Y.P. Wang, *Notopterygium forrestii* H. Wolff and *Notopterygium tenuifolium* Sheh et Pu. The Chinese medicinal herb Qianghuo (QH) refers to the dried rhizomes and roots of *Notopterygium* or broad-leaved *Notopterygium*. The main chemical constituents isolated from QH are volatile oils, coumarins, alkaloids, etc<sup>[2]</sup>. Pharmacological investigations have revealed that QH possesses anti-inflammatory, antibacterial, antioxidant, antiviral, and anticancer effects and has antipyretic and analgesic effects<sup>[3]</sup>. Furthermore, QH has significant effects on the cardiovascular and cerebrovascular systems, digestive system, respiratory system, and central nervous system<sup>[4]</sup>. However, limited research has explored the potential of QH in anticancer therapy, and no attempts have been made to use QH to treat CRC.

B-cell lymphoma 2-interacting mediator of cell death (BIM) was reported to play a pivotal role as a potent proapoptotic protein within the B-cell lymphoma 2 protein family<sup>[5]</sup>. BIM exhibits distinct properties that distinguish it from other BH3-only proteins. Notably, alternative splicing produces multiple BIM isoforms, each possessing varying intrinsic pro-apoptotic activities

Jun-he CHEN, E-mail: aukosakakihara@sina.cn

#Corresponding author, E-mail: wzma@must.edu.mo

\*This study was funded by the Science and Technology Development Fund, Macau SAR (No. 0105/2022/A2 and No. 006/2023/SKL).

and regulatory mechanisms<sup>[5-7]</sup>. Under stress conditions, c-Jun N-terminal kinases phosphorylate BIM Long (BIM L) and BIM Extra Long (BIM EL) isoforms, promoting apoptosis<sup>[8,9]</sup>. However, under unstressed conditions, BIM undergoes phosphorylation and ubiquitination-mediated degradation. Oncogenes use these degradation pathways to inhibit or neutralize BIM, thereby promoting tumor cell survival. Therefore, BIM inhibition has been suggested to be an important target in the tumorigenesis of CRC<sup>[10]</sup>. In this study, we investigated the antitumor activities of QH in CRC and explored its impact on the proapoptotic protein BIM.

## 1 MATERIALS AND METHODS

### 1.1 QH Extracts

The QH extracts were obtained from the China National Institutes for Food and Drug Control (610006). Their quality was detected by high-performance liquid chromatography (HPLC) with reference to the characteristic map of QH chinensis in the 2015 edition of the Chinese Pharmacopoeia.

### 1.2 Cell Culture

The human CRC cell lines HCT116 and Caco-2 were purchased from the American Type Culture Centre (ATCC). HCT116 cells were cultured in Dulbecco's modified Eagle's medium (DMEM), and Caco-2 cells in minimal essential medium (MEM) supplemented with 10% fetal bovine serum and 1% penicillin-streptomycin-glutamine at 37°C in 5% CO<sub>2</sub>. All media, serum, and antibiotics were purchased from Gibco (Thermo Fisher Scientific, USA).

### 1.3 Cell Viability Assay

The sulforhodamine B (SRB) assay was used to assess cell viability as previously described<sup>[11]</sup>. HCT116 cells and Caco-2 cells were seeded into 96-well plates (5000 cells/well), incubated overnight, and subsequently treated with QH at 0, 5, 10, 20, 40, 80 µg/mL for 48 h (dose-response), or at 40 µg/mL for 3, 6, 12, 24, 48 h (time course). After indicated treatment time, 50 µL of 50% trichloroacetic acid was added to the cells, which were subsequently washed with tap water and stained with 100 µL of 0.04% (w/v) SRB. The cells were washed 4 times with 1% acetic acid and then air-dried. Two hundred microliters of 10 mmol/L Tris base solution (pH 10.5) were used to dissolve the bound SRB, and the absorbance at 515 nm was measured.

### 1.4 Colony Formation Assay

HCT116 cells and Caco-2 cells were seeded into 6-well plates (500 cells/well) and incubated overnight. They were then treated with 3 mL of medium containing QH at 0, 2.5, 5, 10, 20, 40 µg/mL for 10 days. The cells were stained with 1 mL of 0.2% crystal violet overnight, washed with 10% PBS, air-dried, and imaged using BIO-RAD ChemiDoc<sup>TM</sup> MP Imaging System.

### 1.5 Apoptosis Assay

HCT116 cells were seeded into 6-well plates (2×10<sup>5</sup> cells/well) and incubated overnight. Subsequently, the cells were treated with 2 mL of medium containing QH

at 10, 20, 40 µg/mL for 48 h. Apoptosis was measured using the PE Annexin V Apoptosis Detection Kit I (BD Biosciences, USA). Briefly, the cells were washed twice with cold PBS and resuspended in 1× binding buffer at a concentration of 1×10<sup>6</sup> cells/mL. A volume of 100 µL of the cell suspension (1×10<sup>5</sup> cells) was transferred to a 5 mL tube. To this, 5 µL of FITC Annexin V and 5 µL PI were added. The cells were gently vortexed and incubated for 15 min at room temperature (25°C) in the dark. Following this, 400 µL of 1× binding buffer was added to each tube. The apoptotic cells were analyzed within 1 h using a CytoFLEX flow cytometer (Beckman Coulter, USA), and the data were analyzed using the CytExpert software (Beckman Coulter, USA).

### 1.6 Cell Cycle Analysis

HCT116 and Caco-2 cells were seeded into 6-well plates (2×10<sup>5</sup> cells/well) and incubated overnight. Subsequently, the cells were treated with 2 mL of medium containing QH at 10, 20, 40 µg/mL for 24 h. After harvesting, the cells were washed twice with precooled PBS and fixed in 70% precooled ethanol at -40°C for 4 h. The cells were then washed with cold PBS and resuspended in 500 µL of a solution containing PI (50 µg/mL) and RNase A (50 µg/mL) for 30 min at room temperature in the dark. Cell cycle analysis was performed using a CytoFLEX flow cytometer (Beckman Coulter, USA), and the data were analyzed using the CytExpert software (Beckman Coulter, USA).

### 1.7 RNA Interference

RNA interference was performed by packaging lentiviruses. Two shRNAs were cloned separately into a linearized pLKO.1-puro. The shRNA and lentiviral packaging vectors were cotransfected into 293T cells (ATCC) using GenJet reagent (SigmaGen, USA) according to the manufacturer's instructions. Lentiviral supernatants were collected 24–48 h after transfection to infect the targeted cells. The knockdown efficiency of the lentivirus was confirmed by Western blotting. The shRNA sequence for BAX (shBAX) was 5'-GACGAACTGGACAGTAACATG-3'.

### 1.8 Immunoblot Analysis

Cells were lysed in RIPA buffer supplemented with protease inhibitor cocktail tablets (cOmplete Mini, Switzerland) and phosphatase inhibitor cocktail tablets (PhosSTOP, Roche Diagnostics). The total protein concentration of the lysates was measured by a direct detection spectrometer (Sigma-Aldrich, USA), and equal amounts of protein were loaded on 8%–12% PAGE gels. The following antibodies were used for the detection of the corresponding proteins: BIM (1:2000, Abcam), β-actin (1:10000, Sigma), BAX (1:1000, Santa Cruz), cleaved-caspase 3 (1:1000, Cell Signaling Technology), and Bcl-2 (1:1000, Cell Signaling Technology).

### 1.9 APC<sup>Min+</sup> Mice

BALB/c-nude mice (aged 5–6 weeks) and APC<sup>Min+</sup> mice (aged 6–8 weeks) were obtained from the Jackson Laboratory (Cambridgeshire, UK). Mice were housed under specific pathogen-free conditions with controlled temperature and humidity and fed on rodent chow (PicoLab

Rodent 20-5035, LabDiet, USA) and reverse osmosis water. The genotype of APC<sup>Min+</sup> mice was confirmed using the KAPA Mouse Genotyping Kit (Roche). The APC<sup>Min+</sup> mouse studies were approved by the Division of Animal Control and Inspection of the Department of Food and Animal Inspection and Control of Macau (Original approved #:130/DICV/DIS/2019, Renewed #: 087/DICV/DIS/2021). All the experimental procedures were conducted within the approved guidelines of the Ethics Review Committee for Animal Research of Macau University of Science & Technology (SKLSOP/AD003/V3/20180619).

Following genotyping, mice aged four weeks were divided into an experimental group and a control group. The mice in the experimental group were administered a daily dose of 0.1 mL 100 mg/mL QH via gavage, while the control group mice received a daily gavage of 0.1 mL 0.5% CMC-Na daily. Body weight measurements were taken weekly. Upon reaching the age of 16 weeks, the mice were euthanized. The whole intestines of the mice were stained with methylene blue, and polyps were counted under a microscope. Pathological sections were prepared from colorectal sections for H&E staining and immunohistochemistry analysis.

### 1.10 Tumor Xenografts

A total of  $5 \times 10^6$  HCT116 cells were subcutaneously implanted into the hind limbs of each nude mouse. Ten days later, the mice were randomly divided into an experimental group and a control group, each containing 5 mice. The experimental group mice were administered a daily dose of 0.1 mL 100 mg/mL QH *via* gavage, while the control group mice received a daily gavage of 0.1 mL 0.5% CMC-Na daily. Gavage was carried out daily, and the tumor size was measured with a digital caliper every 4 days. Four weeks later, the mice were sacrificed, and the tumors were harvested for further measurements. Ten monitoring points of tumor volume in the mice were collected. The average tumor volume was calculated using the following formula: Volume = (width)<sup>2</sup> × length/2. The nude mouse studies were approved by the Division of Animal Control and Inspection of the Department of Food and Animal Inspection and Control of Macau (Original approved #:073/DICV/SIS/2016, Renewed #: 087/DICV/DIS/2021). All the experimental procedures were conducted within the approved guidelines of the Ethics Review Committee for Animal Research of Macau University of Science & Technology (SKLSOP/AD003/V3/20180619).

### 1.11 Histological Examination

Hematoxylin and eosin (H&E) staining and immunohistochemistry were performed using standard procedures with 5- $\mu$ m thick frozen sections for staining. Hematoxylin and eosin dyes were obtained from Dako (Denmark). The colorectum tissues of mice were taken to observe the morphological structure of the lesions with a Leica microscope, and photographed with a supporting camera (DFC310FX, Leica, Germany) and software (Leica Application Suite Version 4.4.0, Switzerland).

### 1.12 Statistical Analysis

Statistically significant differences were analyzed by two-tailed Student's *t*-tests using GraphPad Prism 6.00 (GraphPad Software, USA). The data are presented as the means  $\pm$  SEMs of *n* (*n*  $\geq$  3) determinations. A *P* value of  $<0.05$  was considered to indicate statistical significance.

## 2 RESULTS

### 2.1 QH Inhibits the Viability of CRC Cells

We utilized the SRB assay to evaluate the impact of QH on the proliferation of CRC cells. We observed that QH treatment resulted in a dose-dependent inhibition on CRC cell proliferation. Specifically, the IC<sub>50</sub> values were determined to be 36.14  $\mu$ g/mL for HCT116 cells and 38.68  $\mu$ g/mL for Caco-2 cells (fig. 1A). This inhibitory effect was further substantiated by a time-dependent response observed when both cell lines were treated with QH at a concentration of 40  $\mu$ g/mL (fig. 1B). Additionally, the colony formation assay revealed a substantial reduction in cell survival following QH treatment (fig. 1C). Given that disruption of cell cycle progression is a primary mechanism underlying the inhibition of proliferation, we employed flow cytometry to detect alterations in the cell cycle. Our analysis revealed a cell cycle arrest in the G1 phase for HCT116 cells and in the S phase for Caco-2 cells following QH treatment (fig. 1D).

### 2.2 QH Inhibits Cellular Activity by Inducing Apoptosis

Flow cytometry revealed that a medium concentration (40  $\mu$ g/mL) of QH induced 50% cell apoptosis in HCT116 cells (fig. 2A), which was more remarkable than that in Caco-2 cells (data not shown). Therefore, HCT116 cells were selected for the rest of the study. Additionally, our experiments demonstrated that caspase 3 underwent dose-dependent cleavage (fig. 2B). To validate the apoptotic process, we pretreated cells with the caspase inhibitor Z-VAD for 6 h and conducted apoptosis assays. The results indicated that HCT116 cell apoptosis could be rescued (fig. 2C). Specifically, the proportion of viable cells under QH treatment at a concentration of 40  $\mu$ g/mL exhibited an increase from 54.6% to 70.0% upon pretreatment with Z-VAD.

### 2.3 QH Prevents the Degradation of BIM

Western blot analysis revealed after QH treatment, there was a significant increase in the proapoptotic protein BIM in HCT116 cells (fig. 2B). Notably, BIM undergoes ubiquitination and proteasome-mediated degradation, maintaining a low cellular level under normal conditions<sup>[12]</sup>. Consequently, we hypothesize that the induction of BIM protein by QH could potentially be attributed to the inhibition of the proteasome-mediated degradation pathway. To test this idea, we treated cells with the protein synthesis inhibitor cycloheximide (CHX) for varying durations. QH was found to prevent rapid BIM degradation over time, resulting in BIM accumulation within the cells and a decreased degradation rate (fig. 3A and 3B). We propose that this phenomenon contributes significantly to QH-induced apoptosis in HCT116 cells. Furthermore, considering the ability of BIM to oligomerize BAX, we hypothesize that BAX also plays an important



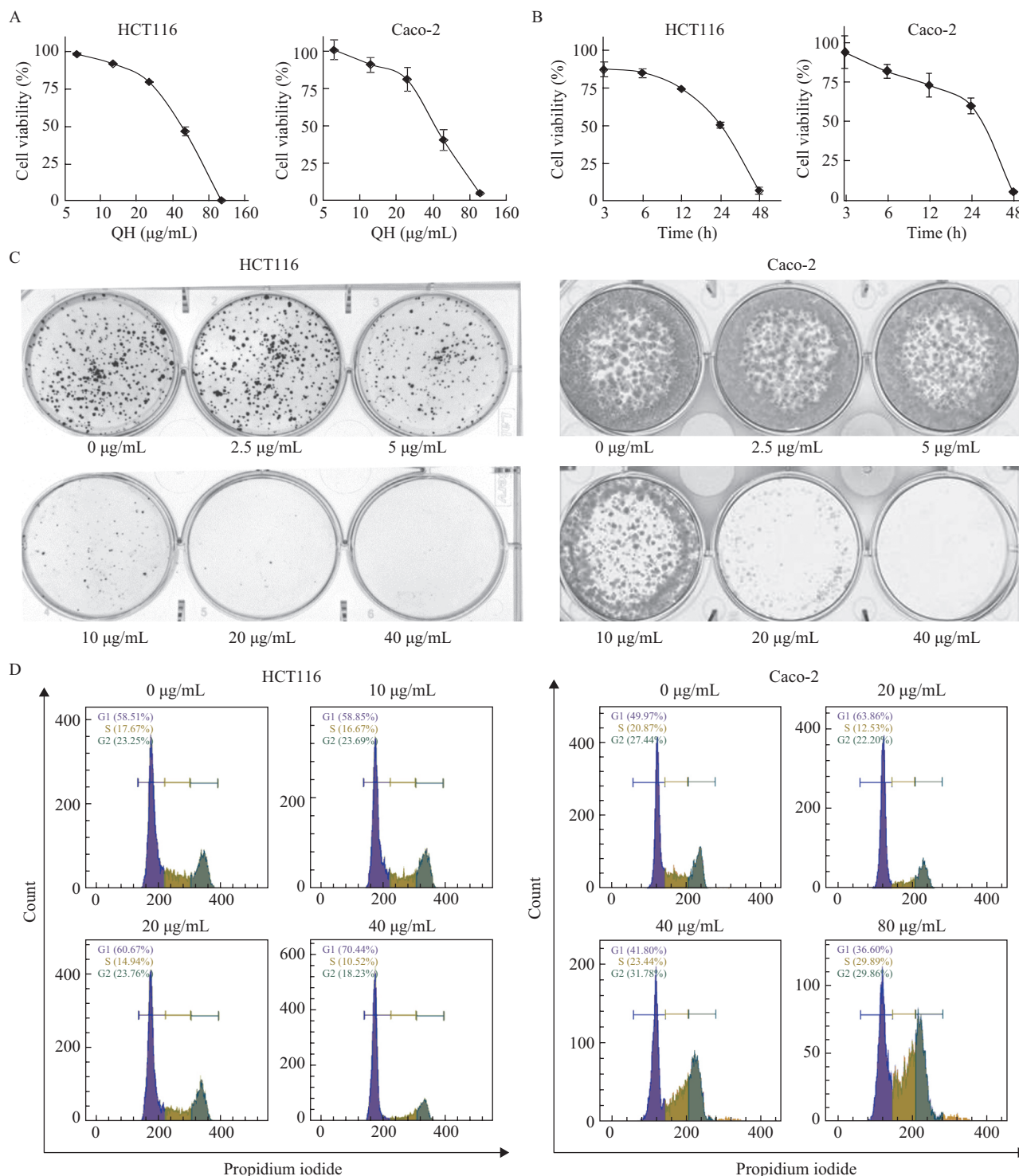


**Fig. 1** Effect of QH on the viability of CRC cell lines

A: In HCT116 and Caco-2 cells, the effect of treatment with different concentrations of QH for 48 h on cell viability was determined by the SRB method. B: the effect of different durations of treatment with a fixed concentration of QH (40 µg/mL) on the viability of the two cell lines; C: The effect on the survival of the two cell lines was examined by a clonogenic assay. D: cell cycle analysis by flow cytometry after QH treatment. Statistical analysis was performed by Student's *t* test (mean±SEM, *n*=3).

role in QH-induced apoptosis<sup>[13]</sup>. To validate this, we employed lentivirus-mediated knockdown of BAX and observed subsequent inhibition of apoptosis, ultimately enabling cell survival (fig. 3C and 3D).

#### 2.4 QH Inhibits Tumors *In Vivo*

By employing a xenograft model, we found that QH administration led to a significant reduction in

tumor volume (fig. 4A). Subsequently, we further tested the *in vivo* antitumor effect of QH using the APC<sup>Min+</sup> spontaneous CRC model. The QH-fed mice exhibited a substantial decrease in the number of intestinal polyps (fig. 4B). Histological examination via H&E staining revealed that the intestinal villus morphology in QH-fed mice closely resembled that in normal mice (fig. 4C



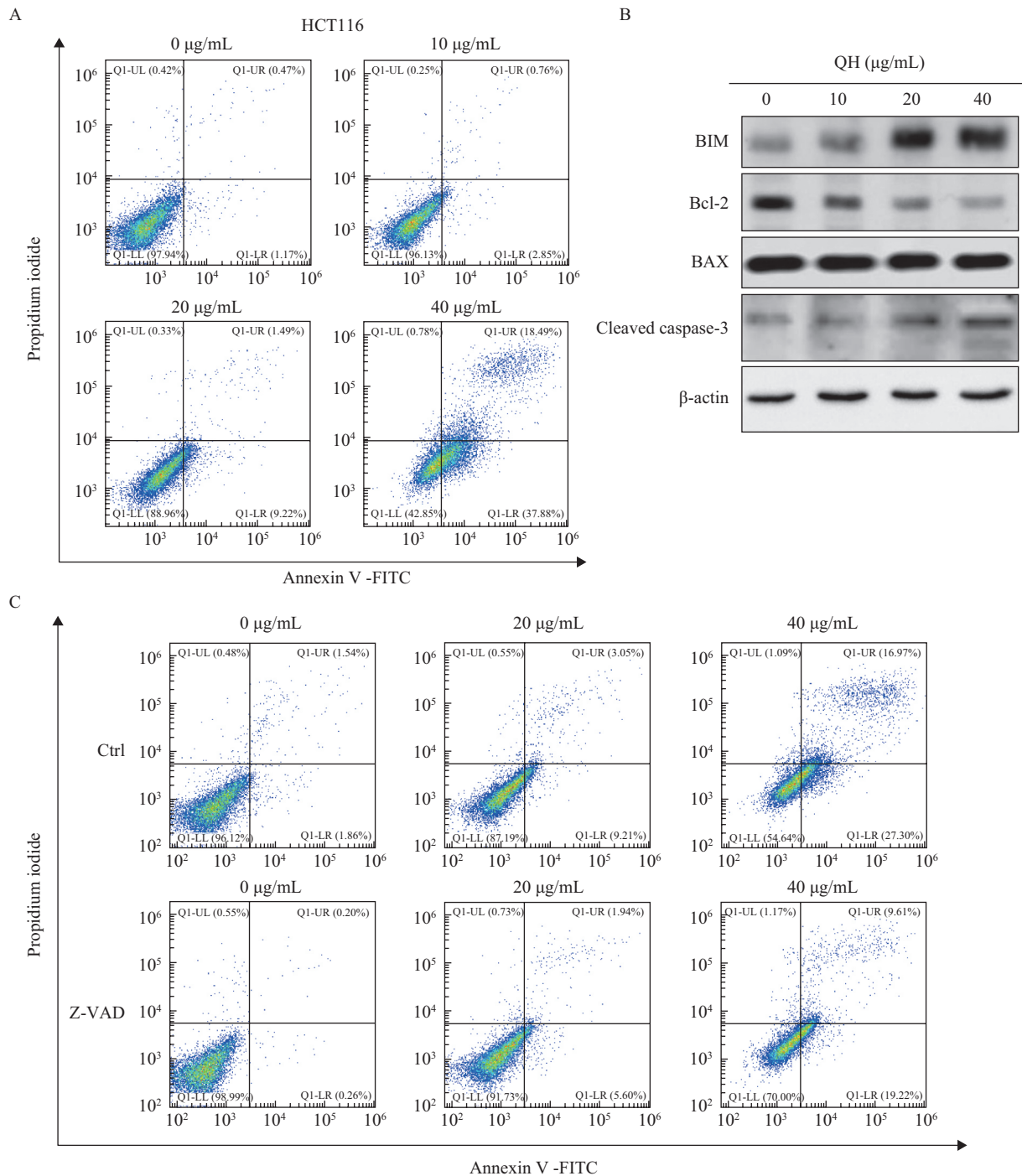


**Fig. 2** Effect of QH on the death pattern of HCT116 cells  
 A: HCT116 cells were treated with QH for 48 h, and the death pattern was determined by flow cytometry. B: The expression of BIM, Bcl-2, BAX, and cleaved caspase-3 was examined by Western blot analysis. β-actin was used as a loading control. C: HCT116 cells were pretreated with 10 µmol/L Z-VAD for 6 h and then treated with QH for 48 h, after which cell apoptosis was detected by flow cytometry.

and 4D). Importantly, QH treatment did not adversely impact overall mouse health, and body weight remained comparable to that of the control group. Moreover, we found that the protein levels of β-catenin and Bcl-2 in the intestine were significantly decreased after QH administration (fig. 5A and 5B).

### 3 DISCUSSION

The anti-cancer properties of QH extract and its

constituents have been previously demonstrated across a variety of cancer cell lines, including hepatocellular carcinoma, breast cancer, pancreatic cancer, lung carcinoma, and ovarian cancer<sup>[14, 15]</sup>. However, its potential effects on CRC cell lines remain to be explored. Moreover, the existing literature is primarily focused on *in vitro* studies, leaving the question of whether QH could inhibit tumor growth *in vivo* largely unanswered. In the present study, we provide evidence of the anti-CRC effects of QH extract in both *in vitro* and *in vivo* settings.

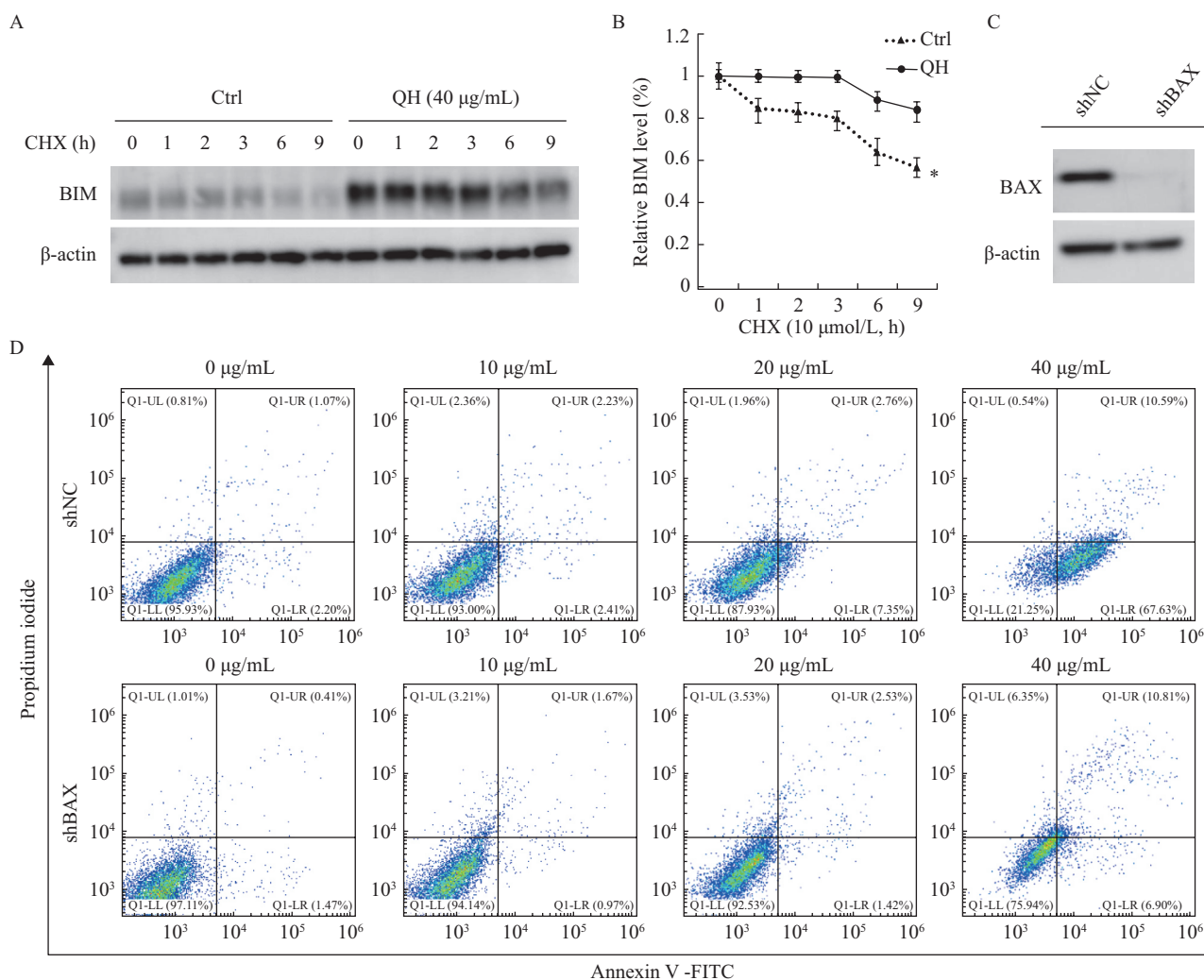


**Fig. 3** QH induces the apoptosis of HCT116 cells through BIM

A: Before sample collection, 20  $\mu\text{g/mL}$  CHX was used for 1, 2, 3, 6, and 9 h, and then, the degradation of BIM was assessed by Western blot analysis. B: The relative BIM level was visualized using line chart. C: After knocking down BAX in HCT116 cells using lentivirus, the expression level of BAX in cells was detected by Western blotting. D: After QH treatment, the apoptosis of HCT116 shBAX cells was detected by flow cytometry, and shNC was used as the experimental control group. Error bars represent  $\pm$  SD ( $n=3$  independent experiments). The data were analyzed using an unpaired Student's  $t$ -test (two-tailed). \* $P<0.05$  vs. QH group. Ctrl: control

In this study, we have demonstrated that the potential mechanism underlying QH-induced apoptosis is primarily through the increase of BIM stability. BIM is typically degraded via the ubiquitin-proteasome pathway under unstressed conditions<sup>[16, 17]</sup>. When activated, BIM binds to pro-survival proteins via its BH3 domain, effectively neutralizing their function<sup>[6]</sup>. This is substantiated by our observation that QH decreased Bcl-2 in a dose-dependent manner (fig. 2B). Additionally, the BH3 domain peptide of BIM can directly bind and induce BAX oligomerization and membrane permeabilization<sup>[18, 19]</sup>. In both scenarios, the apoptosis executioner BAX undergoes conformational changes without altering its overall protein content in the whole-cell lysate. This is consistent with our observations of the unchanged BAX protein levels under QH treatment. However, the complex interplay between BIM, Bcl-2, and BAX, and the potential involvement of other Bcl-2 family members in mediating QH-induced apoptosis warrant further investigation. The activation of the BIM/Bcl-2/BAX pathway eventually triggered the cleavage of

caspase 3, the active form of the protease, which serves as the executioner and marker of apoptosis. Moreover, our findings revealed that pretreatment with the caspase inhibitor Z-VAD effectively rescued QH-induced apoptosis. Taken together, these results suggested that QH induced apoptosis through the regulation of BIM/Bcl-2/BAX/caspase 3 pathway.

Nonetheless, the precise mechanism by which QH enhances the stability of BIM remains to be elucidated. The stability of BIM is governed by several pathways. For instance, the phosphorylation of BIM at Ser169 by the MAPK kinase ERK1/2 is known to expedite its degradation<sup>[8, 20]</sup>. Conversely, the phosphorylation of Bim at Ser83 by protein kinase A (PKA) enhances BIM stabilization<sup>[21]</sup>. The interaction of BIM with dynein light chain 1 (DLC1) protects BIM from proteasomal degradation<sup>[22]</sup>, while its interaction with  $\beta$ -TrCP1, Cyclin B1, or APC<sup>Cdc20</sup> results in the ubiquitination and subsequent degradation of BIM<sup>[23-25]</sup>. Further research is warranted to explore the potential influence of QH on these pathways.

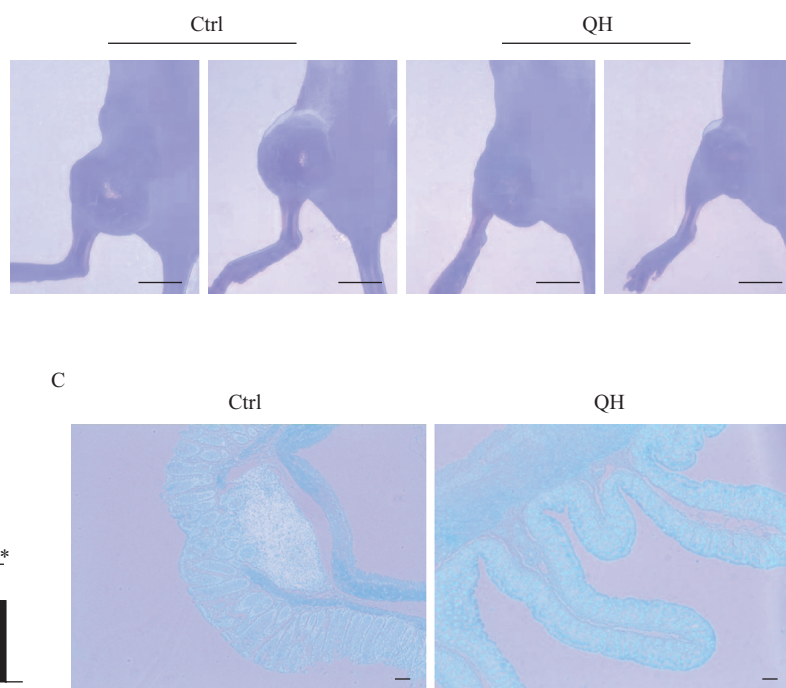
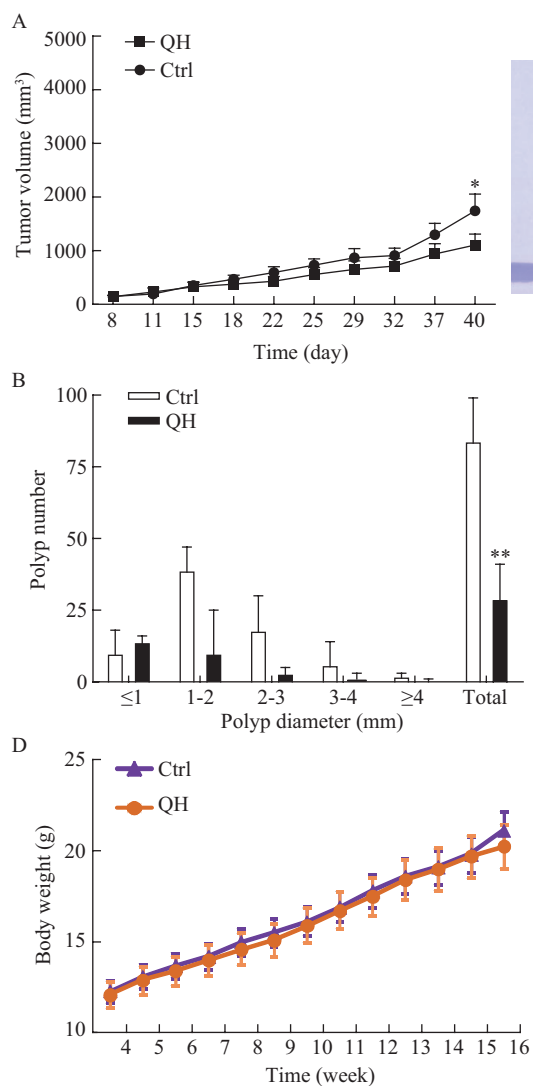


**Fig. 4** QH inhibits tumor proliferation *in vivo*

**A:** Nude mice were implanted with HCT116 cells. After 10 days, QH was administered to the xenograft mice daily. Tumor size was measured with digital calipers on the indicated days. The graph shows tumor growth in the mice. Representative images of xenografts are shown after the mice were sacrificed. Error bars represent  $\pm$ SEMs ( $n=10$  independent experiments). \* $P<0.05$ . Scale bar: 1 cm. **B:** The intestinal polyps of the APC<sup>Min+</sup> mice were counted under an operating microscope after staining with methylene blue. Statistical analysis was performed on the total number of polyps. Error bars represent  $\pm$ SD ( $n=7$  independent experiments). The data were analyzed using an unpaired Student's *t*-test (two-tailed). \*\* $P<0.001$ . **C:** H&E staining of mouse intestine showing polyp morphology. The microscope magnification was 10 $\times$ . Scale bar: 25  $\mu$ m. **D:** The line chart showed the changes in APC<sup>Min+</sup> mice body weight during the experiment. Ctrl: control

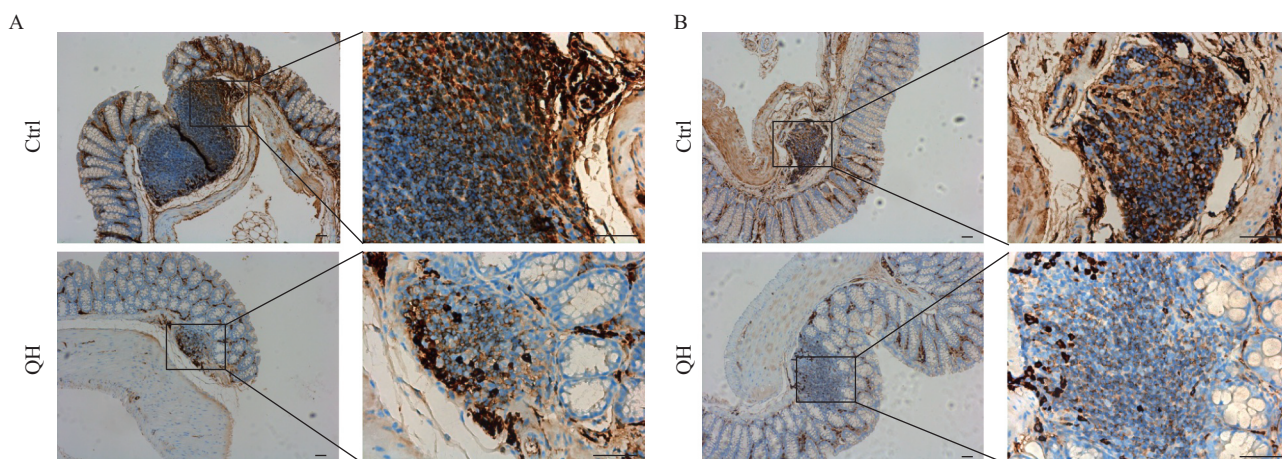


**Fig. 5** QH decreases BIM-associated proteins in the intestinal tissues of APC<sup>Min+</sup> mice

**A:** Immunohistochemical analysis of mouse intestinal polyps was performed using an anti- $\beta$ -catenin antibody. Low magnification, 10 $\times$ ; high magnification, 40 $\times$ . Scale bar: 25  $\mu$ m. **B:** Immunohistochemical analysis of mouse intestinal polyps was performed using an anti-Bcl-2 antibody. Low magnification, 10 $\times$ ; high magnification, 40 $\times$ . Scale bar: 25  $\mu$ m. Ctrl: control

A further unresolved issue pertains to the specific components within QH that contribute to its anti-CRC activities. This is particularly significant given the intricate diversity and complexity of traditional Chinese medicine ingredients. In the case of QH, 4 primary chemical components were analyzed: notopteron, phenethyl

ferulate, iso-impemtorin, and falcarinol. However, the precise component responsible for BIM stabilization within the QH remains elusive. Investigating this matter through approaches such as network pharmacology and experimental validation is crucial for advancing anticancer drug development.



Given the high homology between the mouse and human genomes, along with similarities in anatomy and physiology, mouse models play a crucial role in cancer biology and drug development. Nude mice, while useful for assessing the inhibitory effects of drugs on tumor growth, have limitations in observing early tumor stages, such as primary tumor growth. To address this issue, we used APC<sup>Min+</sup> mice, a genetically engineered mouse model that closely mimics human colon cancer and polyps. This model allows for the observation of intestinal polyp evolution and local proliferation into adenomas without the need for additional chemical induction.

In conclusion, our study demonstrated both *in vitro* and *in vivo* activities of QH extract against CRC by promoting apoptosis *via* stabilization of BIM protein. This highlights the potential of the QH extract as a promising option for treating CRC.

#### Conflict of Interest Statement

The authors declare that there is no conflict of interest with any financial organization or corporation or individual that can inappropriately influence this work.

#### REFERENCES

- Huang J, Lucero-Prisno DE 3rd, Zhang L, *et al.* Updated epidemiology of gastrointestinal cancers in East Asia. *Nat Rev Gastroenterol Hepatol*, 2023,20(5):271-287
- Azietaku JT, Ma H, Yu XA, *et al.* A review of the ethnopharmacology, phytochemistry and pharmacology of *Notopterygium incisum*. *J Ethnopharmacol*, 2017,202:241-255
- Ouyang HF, Wang YQ, Zhao LX, *et al.* Research progress and application analysis of chemical constituents, pharmacological effects, and pharmacokinetics of the endangered medicinal material *Qianghuo*. *Zhongyi Yaoli Yu Linchuang* (Chinese), 2023,14(4):105-111
- Yang CM, Guo JM, Yao TM. Research Progress on Clinical Application and Pharmacological Activity of *Qianghuo* (*Rhizoma Et Radix Notopterygii*). *Shiyong Zhongyi Neike Zazhi* (Chinese), 2022,36(4):25-28
- O'Connor L, Strasser A, O'Reilly LA, *et al.* Bim: a novel member of the Bcl-2 family that promotes apoptosis. *Embo J*, 1998,17(2):384-395
- Chen L, Willis SN, Wei A, *et al.* Differential targeting of prosurvival Bcl-2 proteins by their BH3-only ligands allows complementary apoptotic function. *Mol Cell*, 2005,17(3):393-403
- Mami U, Miyashita T, Shikama Y, *et al.* Molecular cloning and characterization of six novel isoforms of human Bim, a member of the proapoptotic Bcl-2 family. *FEBS Lett*, 2001,509(1):135-141
- Hübner A, Barrett T, Flavell RA, *et al.* Multisite phosphorylation regulates Bim stability and apoptotic activity. *Mol Cell*, 2008,30(4):415-425
- Lei K, Davis RJ. JNK phosphorylation of Bim-related members of the Bcl2 family induces Bax-dependent apoptosis. *Proc Natl Acad Sci U S A*, 2003,100(5):2432-2437
- Greenhough A, Wallam CA, Hicks DJ, *et al.* The proapoptotic BH3-only protein Bim is downregulated in a subset of colorectal cancers and is repressed by antiapoptotic COX-2/PGE(2) signalling in colorectal adenoma cells. *Oncogene*, 2010,29(23):3398-3410
- Vichai V, Kirtikara K. Sulforhodamine B colorimetric assay for cytotoxicity screening. *Nat Protoc*, 2006,1(3):1112-1116
- Gupta I, Singh K, Varshney NK, *et al.* Delineating Crosstalk Mechanisms of the Ubiquitin Proteasome System that Regulate Apoptosis. *Front Cell Dev Biol*, 2018,6:11
- Czabotar PE, Colman PM, Huang DC. Bax activation by Bim? *Cell Death Differ*, 2009,16(9):1187-1191
- Ma LM, Yang JL. Research progress on chemical constituents and pharmacological activities of *Notopterygii Rhizoma et Radix*. *Zhongcaoyao* (Chinese), 2021,52(19):6111-6120
- Guo P, Lang YJ, Zhang GT. Research Progress on Chemical Constituents and Pharmacological Activity of *Notopterygii Rhizoma*. *Zhongchengyao* (Chinese), 2019,41(10):2445-2459
- Sionov RV, Vlahopoulos SA, Granot Z. Regulation of Bim in Health and Disease. *Oncotarget*, 2015,6(27):23058-23134
- Ley R, Balmanno K, Hadfield K, *et al.* Activation of the ERK1/2 signaling pathway promotes phosphorylation and proteasome-dependent degradation of the BH3-only protein, Bim. *J Biol Chem*, 2003,278(21):18811-18816
- Kim H, Tu HC, Ren D, *et al.* Stepwise activation of BAX and BAK by tBID, BIM, and PUMA initiates mitochondrial apoptosis. *Mol Cell*, 2009,36(3):487-499
- Zhang J, Huang K, O'Neill KL, *et al.* Bax/Bak activation in the absence of Bid, Bim, Puma, and p53. *Cell Death Dis*, 2016,7(6):e2266
- Ley R, Ewings KE, Hadfield K, *et al.* Extracellular signal-regulated kinases 1/2 are serum-stimulated "Bim(EL) kinases" that bind to the BH3-only protein Bim(EL) causing its phosphorylation and turnover. *J Biol Chem*, 2004,279(10):8837-8847
- Moujalled D, Weston R, Anderton H, *et al.* Cyclic-AMP-dependent protein kinase A regulates apoptosis by stabilizing the BH3-only protein Bim. *EMBO Rep*, 2011,12(1):77-83
- Puthalakath H, Huang DC, O'Reilly LA, *et al.* The proapoptotic activity of the Bcl-2 family member Bim is regulated by interaction with the dynein motor complex. *Mol Cell*, 1999,3(3):287-296
- Moustafa-Kamal M, Gamache I, Lu Y, *et al.* BimEL is phosphorylated at mitosis by Aurora A and targeted for degradation by  $\beta$ TrCP1. *Cell Death Differ*, 2013,20(10):1393-1403
- Gilley R, Lochhead PA, Balmanno K, *et al.* CDK1, not ERK1/2 or ERK5, is required for mitotic phosphorylation of BIMEL. *Cell Signal*, 2012,24(1):170-180
- Wan L, Tan M, Yang J, *et al.* APC(Cdc20) suppresses apoptosis through targeting Bim for ubiquitination and destruction. *Dev Cell*, 2014,29(4):377-391

(Received Jan. 24, 2024; accepted Apr. 9, 2024)